

First Evidence for Phototropin-Related Blue-Light Receptors in Prokaryotes

Aba Losi,^{*,†} Eugenia Polverini,^{*} Benjamin Quest,[‡] and Wolfgang Gärtner^{†‡}

^{*}Istituto Nazionale per la Fisica della Materia and Department of Physics University of Parma, Parco Area delle Scienze 7/A, 43100 Parma, Italy, [†]Max-Planck-Institut für Strahlenchemie, D-45470 Mülheim an der Ruhr, and [‡]Max-Planck-Institut für Biochemie, D-82152 Martinsried, Germany

ABSTRACT A prokaryotic protein, YtvA from *Bacillus subtilis*, was found to possess a light, oxygen, voltage (LOV) domain sharing high homology with the photoactive, flavin mononucleotide (FMN)-binding LOV domains of phototropins (phot), blue-light photoreceptors for phototropism in higher plants. Computer-based three-dimensional modeling suggests that YtvA-LOV binds FMN in a similar pocket as phot-LOVs. Recombinant YtvA indeed exhibits the same spectroscopical features and blue-light-induced photochemistry as phot-LOVs, with the reversible formation of a blue-shifted photoproduct, assigned to an FMN-cysteine thiol adduct (Thio₃₈₃). By means of laser-flash photolysis and time-resolved optoacoustic experiments, we measured the quantum yield of formation for Thio₃₈₃, $\Phi_{\text{Thio}} = 0.49$, and the enthalpy change, $\Delta H_{\text{Thio}} = 135$ kJ/mol, with respect to the parent state. The formation of Thio₃₈₃ is accompanied by a considerable volume contraction, $\Delta V_{\text{Thio}} = -13.5$ ml/mol. Similar to phot-LOVs, Thio₃₈₃ is formed from the decay of a red-shifted transient species, T₆₅₀, within 2 μ s. In both YtvA and free FMN, this transient has an enthalpy content of ~ 200 kJ/mol, and its formation is accompanied by a small contraction, $\Delta V_{\text{T}} \approx -1.5$ ml/mol, supporting the assignment of T₆₅₀ to the FMN triplet state, as suggested by spectroscopical evidences. These are the first studies indicating that phototropin-related, blue-light receptors may exist also in prokaryotes, besides constituting a steadily growing family in plants.

INTRODUCTION

The phototropin (phot) family includes membrane-associated kinases that undergo autophosphorylation in response to ultraviolet-A (UVA)-blue light and represent the main photoreceptors for phototropism in plants (reviewed in Briggs et al., 2001). The knowledge regarding their occurrence, structure, and unique photochemistry is rapidly growing. Phototropins possess two *N*-terminal photoactive light, oxygen, voltage (LOV) domains, LOV being a subset of the Per-Arnt-Sim (PAS) superfamily (Zhulin et al., 1997), and a *C*-terminal serine/threonine domain. Phototropin LOVs (LOV1 and LOV2) bind an oxydized flavin mononucleotide (FMN) as chromophore (Christie et al., 1999) and, upon blue-light illumination, undergo a photocycle, involving the reversible formation of a FMN-cysteine C4a-thiol adduct, in which FMN is reduced and the cysteine oxidized (Salomon et al., 2000, 2001). The cysteine involved in the formation of the photoadduct is situated in a highly conserved sequence motif, NCRFLQG. Recently, the crystal structure of the LOV2 domain from the *Adiantum* phytochrome/phototropin chimeric photoreceptor phy3 was solved at 2.73-Å resolution, showing also the position of the 16 residues directly interacting with FMN (Crosson and

Moffat, 2001). Other eukaryotic proteins, for which a blue-light-dependent function is known, possess phototropin LOV-like domains where the majority of the flavin-interacting residues are conserved (Crosson and Moffat, 2001 and references therein). Up to now, no such proteins have been reported in bacteria, where, nevertheless, PAS domains as photosensors are well represented by the blue-light yellow protein (PYP), binding *p*-coumaric acid as chromophore (Hoff et al., 1994). The occurrence of phot-like receptors in bacteria would thus be meaningful from the evolutionary point of view and such proteins would constitute a novel type of blue-light photosensors in prokaryotes. In the following, we present theoretical predictions and experimental evidences that YtvA, a *Bacillus subtilis* protein, binds FMN in the same environment of phot-LOVs and undergoes the same photochemistry, with the formation of a blue-shifted species, assigned, by analogy with phot, to a C4a-thiol adduct (referred as Thio₃₈₃). The blue-light-induced reactions of full-length, recombinant YtvA, were studied by means of steady-state spectroscopy, laser-flash photolysis, and laser-induced optoacoustic spectroscopy (LIOAS) (Braslavsky and Heibel, 1992). This approach allowed the measurement of the quantum yield (Φ_i) of the photoinitiated reactions in YtvA as well as enthalpic, ΔH_i , and volumetric changes, ΔV_i , occurring in the subnanosecond-to-microsecond time region. The results show that YtvA undergoes considerable blue-light-induced structural changes on this time domain, concomitant with the formation of Thio₃₈₃. The experimental results reported in this work constitute the first evidence that bacteria possess blue-light receptors showing phot-like

Submitted November 21, 2001 and accepted for publication January 11, 2002.

Dedicated to Silvia E. Braslavsky on her 60th birthday.

Address reprint requests to A. Losi, Max-Planck-Institut für Strahlenchemie, D-45470 Mülheim an der Ruhr, Germany, 45470. Tel: 49-208-306-3694; Fax: 49-208-306-3951; E-mail: aba@mpi-muelheim.mpg.de.

© 2002 by the Biophysical Society

0006-3495/02/05/2627/08 \$2.00

photochemistry, despite the fact that the role of such photosensors in vivo is still undetermined.

MATERIALS AND METHODS

Protein expression and purification

The *ytaA* gene (GeneBank accession number: AAC00382) was cloned from *B. subtilis* DNA (kindly provided by K.-E. Jäger, University Bochum, Germany) into the pET28A plasmid (Novagen-Merck, Darmstadt, Germany), after being furnished at the 3' end with an oligonucleotide encoding for a thrombin site and a His₆-tag. His-tagged YtaA was expressed in *Escherichia coli* strain BL21 (Stratagene, Amsterdam, The Netherlands). Isopropyl-β-D-thiogalactopyranoside (IPTG) (BioMol, Hamburg, Germany)-induced expression, followed by purification of the recombinant protein (affinity chromatography on Talon (Qiagen, Hilden, Germany), yielded homogeneous material for spectroscopy. The bound FMN was characterized by thin layer chromatography (TLC) on Silica Gel 60 F₂₅₄ sheets (Merck, Darmstadt, Germany), after protein denaturation and chromatophore separation as described in (Christie et al., 1999).

Three-dimensional modeling

The search for sequence homologs of phototropin LOV domains and the pairwise alignment were performed at the European Bioinformatics Institute) using the BLAST network service (Swiss Institute of Bioinformatics) (Altschul et al., 1997). The three-dimensional (3D) structure of YtaA-LOV was built using the tools available in the What If (Vriend, 1990) software and the phy3-LOV2 (chain A) structure as template. The crystal structure of phy3-LOV2 was obtained from the Brookhaven Protein Data Bank (entry ID code 1G28). A minimization program was carried out with the Gromos96 force field implementation of SwissPdbViewer (van Gunsteren et al., 1996).

Instrumentation

Absorption spectra were recorded with a UV-2102PC spectrophotometer (Shimadzu Germany, Duisburg, Germany). Steady-state fluorescence measurements were performed with a Spex Fluorolog spectrofluorometer. FMN (Fluka, Neu-Ulm, Germany) was used as a standard ($\Phi_F = 0.26$ (van den Berg et al., 2001)) to measure the fluorescence quantum yield of YtaA.

For the LIOAS experiments, excitation at 450 nm was achieved by pumping the frequency-tripled pulse of an Nd:YAG laser (SL 456G, 6-ns pulse duration, 355 nm, Spectron Laser System, Rugby, United Kingdom) into a beta barium borate optical parametric oscillator (OPO-C-355, band-width 420–515 nm, Laser Technik Vertriebs GmbH, Ertestadt-Friesheim, Germany) as previously described (Losi et al., 2000). The beam was shaped by a 0.5 × 6 mm slit, allowing a time resolution of ~30 ns by using deconvolution techniques (Rudzki et al., 1985). The experiments were performed in the linear regime of amplitude versus laser fluence, which was up to 35 μJ/pulse. The total incident energy normally used was ~20 μJ/pulse (fluence = 666 μJ/cm²). New coccine (Fluka) was used as calorimetric reference (Abbruzzetti et al., 1999). The time evolution of the pressure wave was assumed to be a sum of monoexponential functions. The deconvolution analysis yielded the fractional amplitudes (ϕ_i) and the lifetimes (τ_i) of the transients (Sound Analysis 3000, Quantum Northwest Inc., Spokane, WA). The time window was between 20 ns and 5 μs. To separate the fraction of energy released as heat (α_i) and the reaction volume

change (ΔV_i) of the *i*th step, occurring with quantum yield Φ_i (Braslavsky and Heibel, 1992; Rudzki-Small et al., 1992), we used

$$\phi_i = \alpha_i + \Phi_i \frac{\Delta V_i}{E_\lambda} \frac{c_p \rho}{\beta}, \quad (1)$$

where E_λ is the molar excitation energy, $\beta = (\partial V / \partial T)_p / V$ is the volume expansion coefficient, c_p is the heat capacity at constant pressure, and ρ is the mass density of the solvent. The variation in $c_p \rho / \beta$ was achieved by varying the temperature, according to the “several temperatures” method (van Brederode et al., 1995). The “two temperature” method (Malkin et al., 1994) was also applied to check the possible dependence of ΔV_i from temperature: the sample waveform was acquired at a temperature for which heat transport is zero, $T_{\beta=0}$ (3.1°C in this case), and at a slightly higher temperature, $T_{\beta>0}$ (6°C here). At $T_{\beta=0}$ the LIOAS signal is only due to ΔV_i . The reference for deconvolution was recorded at $T_{\beta>0}$, and α_i and ΔV_i were then derived by

$$\Phi_i \Delta V_i = \phi_i|_{T_{\beta=0}} \times E_\lambda \frac{\beta}{c_p \rho} \Big|_{T_{\beta=0}}, \quad (2a)$$

$$\alpha_i = \phi_i|_{T_{\beta>0}} - \phi_i|_{T_{\beta=0}}. \quad (2b)$$

Flash photolysis measurements were performed with the equipment previously described (Ruddat et al., 1997) using 450 nm and 475 excitation. 5,10,15,20-tetrakis-(4-sulfonatophenyl)-porphyrin (TPPS, Porphyrin Products Inc., Logan, Utah) was used as an actinometer, with a quantum yield of triplet production measured at 460 nm, Φ_T TPPS = 0.6, and a triplet-triplet absorption coefficient, $\epsilon_{460,TPPS} = 47,000 \text{ M}^{-1} \text{cm}^{-1}$ (van Brederode et al., 1995).

RESULTS

Homology searching and 3D modeling

A BLAST (Altschul et al., 1997) search through public databases found that phot-like, LOV domains are present in three bacterial proteins, numbering (as in the SwissProt-Trembl database): O34627 (YtaA) in *B. subtilis*, Q9ABE3 in *Caulobacter crescentus*, Q55576 in *Synechocystis* sp strain PCC 6803, all with unknown or poorly characterized function. In particular, the LOV domain of YtaA from *B. subtilis* (aa 25–126), a 261-aa protein, shows the largest percentage of consensus sequences, the largest homology in the residues that interact with FMN in phy3-LOV2, and the smallest degree of gaps. The homology is for some cases, e.g., phot1-LOV2 from *Arabidopsis thaliana*, as large as 86%.

The pairwise homology between the YtaA-LOV and the phy3-LOV2 domains (amino acids 25–126 for YtaA and 929–1032 for phy3) is 69%, including only the identities and the high-similarity residues (Fig. 1), although it grows to 76% if the low-similarity residues are considered also. To construct the model of YtaA-LOV, the coordinates of the backbone atoms were generated using those of the template model in the regions with identical sequence length. The two amino acids at the extremes of the gap in the YtaA-LOV sequence were joined with the paste tool in the What If software (Vriend, 1990). Given that the gap is positioned at the end of a narrow and quite long loop, the joining

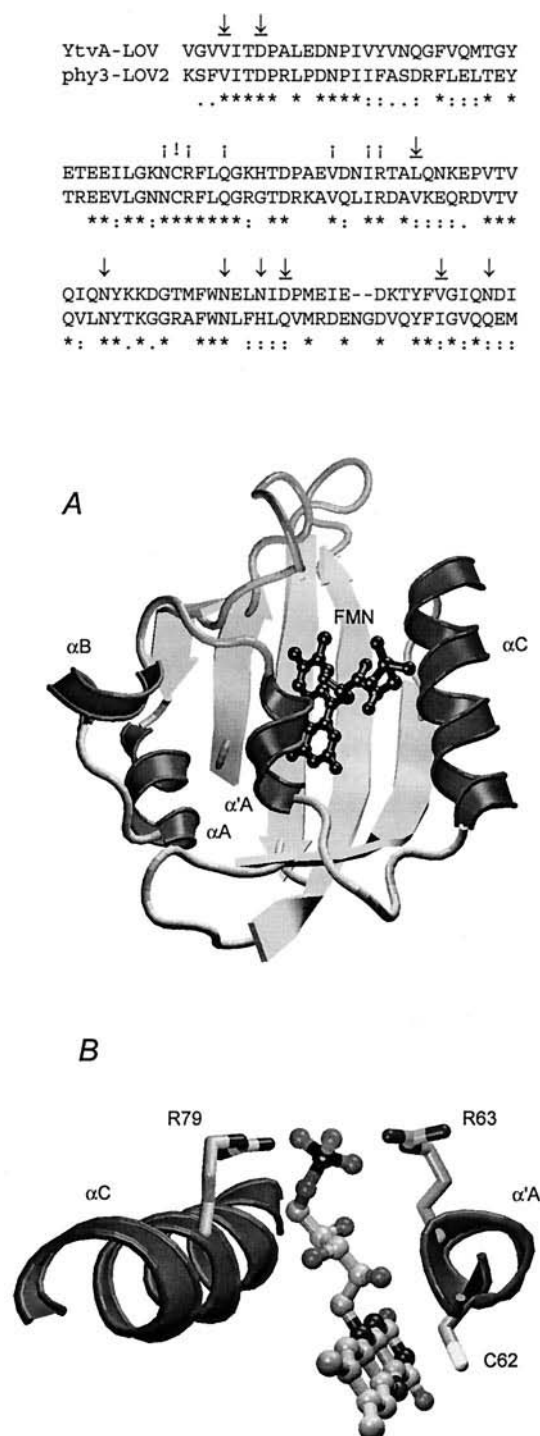


FIGURE 1 *Top*, Best pairwise alignment of YtvA-LOV with phy3-LOV2: *, identity; :, high similarity; ., low similarity. The residues interacting with FMN in phy3-LOV2 (Crosson and Moffat, 2001) are indicated with arrows. ↓, Interactions with the ribityl chain; !, photochemically active cysteine; ↓, hydrophobic pocket around the dimethyl benzyl ring of FMN; ↓, interactions with the isoalloxazine ring. (A) Structural model of YtvA-LOV domain. In dark gray are the four helix-motifs with the central α' A helix, and the β scaffold is in light gray. The FMN cofactor is shown in black. The figure was generated with VMD. (B) The two helices forming the sandwich-like pocket that contains the three residues C62, R63, and R79 (in a stick representation). The FMN chromophore is represented

changes neither the global nor the local molecular conformation. Side-chain conformations were generated using the rotamer library also included in What If. Bumps in the model were then adjusted with small rotations around side-chain torsion angles, and the structure was regularized for correct bond length and angles. After minimization, the refined model was evaluated using the What If tools for protein structure verification, which resulted in very good quality. To insert an FMN molecule into the flavin-binding pocket, we overlapped the YtvA-LOV and the phy3-LOV2 structures by means of the tool present in SwissPdbViewer software, to bring them into the same coordinates frame. Looking at the atomic distance of the more relevant residue (e.g., the sulfur atom of C62 of YtvA being 4.2 Å from C4 atom of FMN, as in the phy3-LOV2 domain) the position of the ligand was found to be reliable, allowing the characterization of the flavin-binding pocket and the FMN environment. The structure of YtvA-LOV exhibits the characteristic PAS domain fold, a pocket including the helix-turn-helix α A/ α B and the helical connector α C as walls, and a five-stranded β scaffold as a floor (Fig. 1). A key region of secondary structure that varies in known PAS structures is the helix α' A (Crosson and Moffat, 2001). α' A is a single turn of a 3_{10} helix that comprises the NCRFLQG consensus sequence including C62 in YtvA. The position of C62 that flanks the face of the flavin ring is identical to C966 in phy3-LOV2. The α' A helix lays in a central position exactly on top of the binding pocket and is connected to the other two helix patterns (α A/ α B and α C) by means of two long and flexible loops. The fact that just α' A contains the essential Cys residue suggests an active role for this helix in the structural changes that occur upon formation of the photoadduct (see Discussion below).

The residues interacting with the ribityl chain of FMN, highlighted in Fig. 1, are all polar and conserved and are located in the α' A and α C helices that surround the ribityl chain in a sandwich-like arrangement. The two helices are amphiphilic and expose their polar side to the ribityl chain. The phosphate group that protrudes from the two helices at the surface of the molecule interacts strongly with the guanidinium groups of R63 and R79 presumably forming salt bridges because of the short distance (2.7 Å). Notably, they are the only two arginine residues in the YtvA-LOV sequence and they are not conserved in PAS domains binding other cofactors (Crosson and Moffat, 2001). The residues that, from the alignment with phy3-LOV2, are supposed to form a hydrophobic pocket around the diethyl benzyl ring, are well positioned in the β scaffold surrounding the ring, even if

in ball and stick. The gray tones in the residues and in the FMN correspond to the different elements: carbon is light gray, oxygen is gray, nitrogen is dark gray, and phosphorus is black.

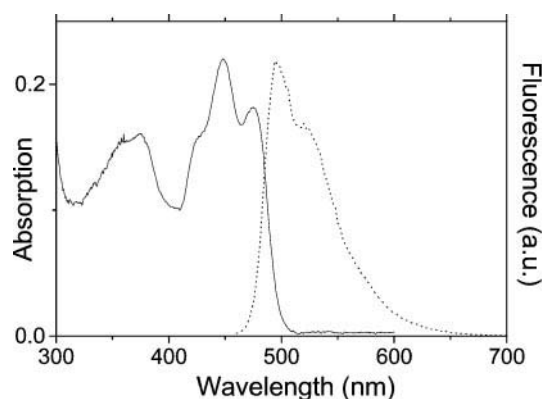


FIGURE 2 Absorption (*left*) and fluorescence (450 nm excitation) spectra of purified YtvA, at 20°C, in 10 mM phosphate buffer, pH = 8, 10 mM NaCl. The fluorescence spectrum is normalized to absorption to evidence the E_{00} level (246.5 kJ/mol, 485 nm).

not all of them are conserved. Also, the residues that surround the isoalloxazine ring lay in the scaffold, and they are all polar with the exception of L106 that, in fact, flanks the ring.

Photochemistry of purified YtvA

Steady-state spectroscopy and photolysis

Cloning of YtvA into an *E. coli* expression vector, after being furnished with a C-terminal His₆-tag yielded, upon IPTG induction, the recombinant protein in good yield and in high purity after affinity purification. In agreement with the above modeling, recombinant YtvA exhibits the same spectroscopical characteristics of phot-LOV domains (Christie et al., 1999; Salomon et al., 2000), with absorption peaks at 375, 449, and 475 nm and a sharp vibrational structure (Fig. 2). The fluorescence maximum is at 496 nm, with a shoulder at 523 nm. The value of Φ_F is 0.22 at 20°C, with only little temperature dependence ($\Phi_F = 0.25$ at 3°C). The spectroscopic data and the 3D modeling allow a conclusion that YtvA, like phot-LOVs, incorporates FMN as a chromophore, in a similarly hydrophobic environment. Accordingly, TLC analysis showed that pure FMN and the YtvA isolated chromophore, upon protein denaturation, have the same mobility relative to the solvent front, whereas riboflavin and flavin adenin dinucleotide behave very differently (Christie et al., 1999).

Blue-light irradiation results in the reversible bleaching of the parent state and in the formation of a photoproduct absorbing maximally at 383 nm, which we assign, by similarity with phot1-LOVs, to the formation of a C4a-thiol adduct (Salomon et al., 2000; Salomon et al., 2001), referred to as Thio₃₈₃. The conversion into Thio₃₈₃ shows three isosbestic points (330, 386, and 409 nm), very similar to *Avena sativa* phot1-LOV2 (Salomon et al., 2000) (Fig. 3). As in phot1-LOV domains (Christie et al., 1999; Salomon et

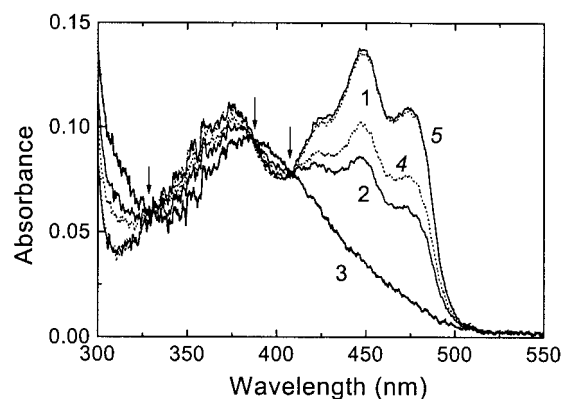


FIGURE 3 Light-induced reaction of recombinant YtvA in 10 mM phosphate buffer, pH 8, 10 mM NaCl. Starting from the parent state (*trace 1*), the protein was flashed for 300 times with laser pulses (450 nm, laser fluence 1 mJ/cm²) until conversion of the chromoprotein into the photoproduct. Trace 2 shows partial conversion after 60 flashes. The arrows indicate the three isosbestic points (330, 386, and 409 nm). The dotted curves 4 and 5 represent the thermally-driven reformation of the parent state after 30 and 120 min (superimposed to the parent state)

al., 2000), the conversion into the photoproduct results in loss of fluorescence: for the species corresponding to curve 3 in Fig. 3, only 5% of the original fluorescence is observed, indicating that curve 3 is an almost pure absorption spectrum for Thio₃₈₃.

Quantum yield determination

Laser flash photolysis measurements ($\lambda_{ex} = 475$ or 450 nm), reveal, similar to phot1-LOV2 (Swartz et al., 2001), the formation of a red-shifted intermediate, T₆₅₀, decaying with a lifetime of 1.6 μ s at 20°C (Fig. 4). Concomitant with the fast, unresolved formation of this species, the parent state shows a maximum bleaching at 450 nm. Assuming that T₆₅₀ absorbs negligibly at this wavelength and by comparing with the maximum amplitude of the triplet-to-triplet absorption of TPPS (van Brederode et al., 1995) we calculated that $\Phi_T = 0.62$. The molar absorption coefficient of YtvA at 450 nm was taken equal to that of FMN, $\epsilon_{450} = 12,500 \text{ M}^{-1}\text{cm}^{-1}$ (van den Berg et al., 2001), an assumption certainly introducing an error in the quantum yields determination. In contrast, YtvA is not as prompt to acid denaturation as LOV domains (Christie et al., 1999) and a variable fraction of the chromophore appears to remain bound to the protein (most probably in the reduced, covalently bound form), rendering very difficult and imprecise the determination of the molar absorption coefficient. Therefore, as a first approach, we decided to use the molar absorption coefficient of free FMN. From the bleaching at 450 nm after the decay of T₆₅₀, it is then possible to determine the quantum yield of formation for the Thio₃₈₃ adduct, $\Phi_{Thio} = 0.49 \pm 0.1$. In this case, we took into account the filter effect exerted by absorption of Thio₃₈₃ at

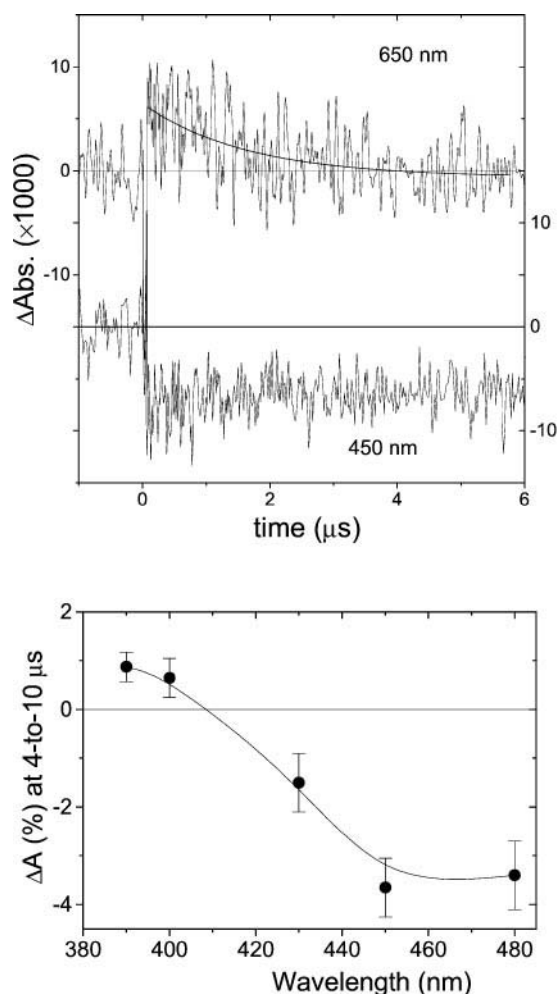


FIGURE 4 *Top*, Single shot, laser-flash induced absorption changes of recombinant YtvA, $\lambda_{\text{ex}} = 475$ nm (20°C). The probe-beam at 650 nm detects the rise (unresolved, <30 ns) and the decay of the red-shifted transient, T_{650} . The monoexponential fitting (also shown in the figure), showed a decay lifetime of 1.6 μs . Detection at 450 nm shows the bleaching of the parent state. The laser fluence was 900 $\mu\text{J}/\text{cm}^2$. *Bottom*, Transient absorption changes, relative to the parent state, as detected between 4 and 10 μs after the laser pulse (excitation was at 450 nm in the case of 475 nm detection). The profile resembles the absorption spectrum of the photoproduct in Fig. 3, despite the very small amplitude of the signals.

450 nm ($\epsilon_{450} = 3240 \text{ M}^{-1} \text{cm}^{-1}$). The direct detection of the photoproduct is quite difficult, given the large overlap between the absorption spectra (Fig. 3). Nevertheless, by recording the relative change in absorption (with respect to the parent state) after the decay of T_{650} (between 4 and 10 μs after the laser flash) at different wavelengths, it is possible to recover a profile that resembles the spectrum of the T_{383} (Fig. 4, *bottom*). It can therefore be concluded that Thio_{383} is formed upon decaying of T_{650} .

Enthalpy and conformational changes

LIOAS experiments gave the results reported in Table 1,

TABLE 1 LIOAS results for YtvA and FMN*

	YtvA	FMN
α_1	0.35 ± 0.04	0.33 ± 0.02
$\Phi_1 \Delta V_1$ (ml/mol)	-0.92 ± 0.11	-1 ± 0.05
α_2	0.21 ± 0.13	0.09 ± 0.02
$\Phi_2 \Delta V_2$ (ml/mol)	-5.7 ± 0.5	$+0.62 \pm 0.1$
τ_2 (μs) at 20°C	1.7 ± 0.2	0.9 ± 0.1
Φ_T (lower limit)	≥ 0.5	≥ 0.5

*The results are an average between several-temperature and two-temperature experiments, Eqs. 1 and 2a,b.

essentially the same with the several-temperatures and two-temperatures method (difference within 10%), showing that, within the small temperature range used (3–20°C) the photophysics of the system does not appreciably change, in agreement with the fluorescence results. LIOAS data for FMN under the same conditions are also reported in Table 1. Each waveform was satisfactorily fitted with a two-exponential function. α_1 and $\Phi_1 \Delta V_1$ (Eq. 1) correspond to the fast processes occurring within 30 ns after the laser pulse, globally assigned to the formation of T_{650} . On the basis of the above reported kinetics, we assign α_2 and $\Phi_2 \Delta V_2$ to the decay of T_{650} into Thio_{383} . For FMN, the prompt process is assigned to the triplet state formation (Sakai et al., 1996; van den Berg et al., 2001). Similar data are obtained for this step for FMN and YtvA. On the basis of energy balance considerations, α_1 is related to the enthalpy stored in the T_{650} (triplet state for FMN) species as

$$\Phi_T \frac{\Delta H_T}{E_\lambda} = 1 - \alpha_1 - \Phi_F \frac{E_F}{E_\lambda}, \quad (3)$$

where E_F is the average energy for the fluorescence emission (232 kJ/mol for YtvA, 221 kJ/mol for FMN). From this relation, we can establish a lower limit for Φ_T by taking the E_{00} energy (246.5 kJ/mol for YtvA, 243 kJ/mol for FMN), as an upper limit for ΔH_T . In both cases $\Phi_T \geq 0.5$, in agreement with the reported values for FMN (average = 0.6 as taken in van den Berg et al. (2001)) and with our value of 0.62 for YtvA (see above). By Eq. 3, we can thus calculate that, in both cases, $\Delta H_T \approx 200$ kJ/mol and $\Delta V_T \approx -1.5$ ml/mol (Table 2).

TABLE 2 Formation quantum yield for T_{650} (Φ_T , triplet state for FMN), for Thio_{383} (Φ_{Thio}) and the corresponding enthalpy (ΔH_i) and volume changes and (ΔV_i)

	YtvA	FMN
Φ_T	0.62 ± 0.1	0.60 ± 0.1
ΔH_T (kJ/mol)*	197 ± 32	203 ± 34
ΔV_T (ml/mol)	-1.5 ± 0.3	-1.7 ± 0.3
Φ_{Thio}	0.49 ± 0.1	—
ΔV_{Thio} (ml/mol)†	-13.5 ± 2.5	—
ΔH_{Thio} (kJ/mol)†	136 ± 65	—

*Eq. 3.

†Eq. 4.

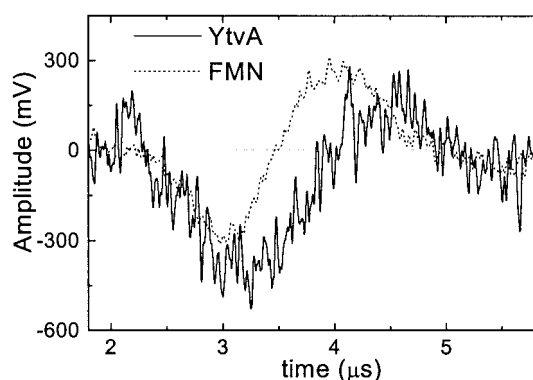


FIGURE 5 LIOAS signal of YtvA and FMN at $T_{\beta=0} = 3.1^\circ\text{C}$ after 450 nm excitation. At this temperature, the signal from the reference compound is zero, i.e., the signal has no thermal contribution and is only due to structural volume changes. For YtvA, five shots were averaged to give a LIOAS waveform.

Instead, the time-resolved step differs dramatically in the two cases (Table 1 and Fig. 5). It is associated with a quite large contraction for YtvA and a small expansion for FMN. The corresponding lifetime is poorly temperature dependent for YtvA, whereas, for FMN, the Arrhenius plot is linear with an activation energy equal to 50 kJ/mol (data not shown). The fraction of released heat, α_2 , is considerably larger in YtvA and can be expressed by the relation,

$$\alpha_2 = \Phi_T \frac{\Delta H_T}{E_\lambda} - \Phi_{\text{Thio}} \frac{\Delta H_{\text{Thio}}}{E_\lambda}. \quad (4)$$

Taken together, these data, and with $\Phi_{\text{Thio}} = 0.49 \pm 0.1$, give an enthalpy content $\Delta H_{\text{Thio}} = (136 \pm 65)$ kJ/mol and a total volume change $\Delta V_{\text{Thio}} = (-13.5 \pm 2.5)$ ml/mol (-22.4 \AA^3), with respect to the parent state (Table 2).

DISCUSSION

Theoretical predictions, based on 3D modeling of YtvA-LOV, and experimental results show that recombinant YtvA, a bacterial protein from *B. subtilis*, binds the same chromophore and undergoes the same photochemistry as LOV domains from plant phototropins (Christie et al., 1999; Salomon et al., 2000). In both chromoproteins, a blue-shifted photoproduct, Thio₃₈₃, is formed upon the decay of a red-shifted transient state, T₆₅₀. Thio₃₈₃ reverts spontaneously to the parent state, albeit the full recovery is much slower in YtvA, and takes ~ 2 h at room temperature (Fig. 3). The extra-stabilization of Thio₃₈₃ may be because YtvA has been expressed as a full-length 261-aa protein, contrary to isolated phot-LOV domains (~ 100 – 110 aa). On the basis of spectroscopical analogies, it was proposed that the red-shifted primary intermediate, in phot1-LOV2 domain, is an FMN excited triplet state (Swartz et al., 2001). The LIOAS data presented here for T₆₅₀, with similar values of ΔH_T and ΔV_T for free FMN and YtvA, are consistent with this

hypothesis. At 20°C , the decay of T₆₅₀ occurs, in YtvA, with an apparent time constant of $1.6 \mu\text{s}$ (see above) and, in the LOV2 domain from oat phot1, of $2 \mu\text{s}$ (Swartz et al., 2001). Most important, the decay of T₆₅₀ into T₃₈₃ is accompanied in YtvA by a considerably large contraction, $\Delta V_{\text{Thio}} = (-13.5 \pm 2.5)$ ml/mol, indicating that the protein undergoes a substantial light-induced structural rearrangement. Similar LIOAS results have been obtained for purified phot-LOV domains (A. Losi et al., in preparation).

The values of $\Delta H_{\text{Thio}} = 136$ kJ/mol and $\Delta V_{\text{Thio}} = -13.5$, are comparable to those measured for PYP upon the formation of the first stable intermediate, pR ($\Delta H_{\text{pR}} = 120$ kJ/mol and $\Delta V_{\text{pR}} = -14$ ml/mol), after isomerization of the *p*-coumaric acid chromophore (van Brederode et al., 1995). In both proteins, the photoreaction takes place in a PAS domain, displaying basically the same folding (Crosson and Moffat, 2001, and Fig. 1), with the chromophore covalently bound, in PYP, to a cysteine residue located in the $\alpha'A$ helix, via a thioester bond (Borgstahl et al., 1995). In phototropin-LOV domains and in YtvA, the cysteine participating in the light-induced reaction is located in the same helix. It is thus conceivable that the main conformational changes in the peptide skeleton occur in this region, due to the strong microenvironment reorganization imposed, in PYP, from chromophore isomerization, and, in the LOV domains, from the formation of a covalent bond. Recently, NMR experiments on *A. sativa* phot1-LOV2 domain, showed that, upon formation of the photoproduct, major changes in the chemical shifts occur in the isoalloxazine ring of FMN (Salomon et al., 2001), as expected from the formation of a covalent adduct. In addition, also the ribityl side-chain carbon atoms and the phosphate residue of FMN undergo substantial chemical-shift changes, indicating conformational changes around the polar chain of the chromophore (Salomon et al., 2001) that strongly interacts with the $\alpha'A$ helix. This region of the protein, both in LOV domains and in PYP, seems thus the best candidate to undergo large conformational changes as a prerequisite for light-to-signal transduction. In YtvA-LOV domain, the presence of two long loops connecting $\alpha'A$ to the other two helical segments (see above and Fig. 1), should confer large flexibility to the protein skeleton in this region.

The question remains of how the light-signal transduction may occur. YtvA has a unique domain organization: downstream from the LOV, a sulfate transporters antisigma (STAS)-factor antagonists (Aravind and Koonin, 2000) domain extends from residue 147 to 258. The STAS domains are found in the C-terminus of eukaryotic sulfate transporters, bacterial anti-sigma factor antagonists and σ^B activation regulators. It has been suggested that STAS have a general NTP binding function (Aravind and Koonin, 2000). This feature is shared between YtvA and phototropins (ATP-binding signature, e.g., aa 670–694 of *Arabidopsis* phot1 (INTERPRO database)) whereas, the Ser/Thr kinase motif is not found in YtvA. Actually YtvA appears to be a


```

At phot1 475 KNFVITDPRLPDNP IIFASDSFLELTEYSREEIL
YtvA      25 VGVVITDPALEDNP IIVVNQGFVQMTGYETEEIL
          ..***** * *****:::..*:::* *.. ****

GRNCRFLQGPETDLTTVKIRNAIDNQTEVTQVLINITYKSGKKFWNI
GKNCRFLQGKHTDPAEVDNIRTALQNKPEVTVQIQNYKKDGTMEFWE
*:***** .*: *: :*:*:*:*:*: *****: **.*. ***

FHLQPMRDQKGEVQYFIGVQLDGSKHVEPVRNVIEETAVKEGEDLVK
LNIDPMEIE--DKTYFVGIQNDITKQKE-YEKLEDSLTEIT--ALS
:::*. : : *::*: * :*: * :*:*:*: : :

KTAVNIDEAVRELPDAN-MTPEDLWANHSKVHVCKPHRKDSPPIWAI
TPIVIRNGISALPIVGNLTERFNSIVCTLTNLSTSKDDYLIIDL
.. * * : : * * . : * * : : : : : : * * . * :

QKVLSEGEPIGLKHF KPVKPLGSGDTGSVHLVELVGTDQLFAMK
SGLAQVNEQTADQIFKLSHLLKL--TG-TELI-ITGIKPELAMK
. : : . * . : * * : * ** .*: :.* . :***

```

FIGURE 6 Best alignment of YtvA and *Arabidopsis* phot1, in the region composed of the LOV (**bold**) domain plus the NTP-binding signature (*italics*) for the former and LOV2 plus the ATP binding-signature for the latter. The homology, including high and low similarity, is 70%. The region covers almost entirely YtvA sequence (209 aa out of 261).

fragment of phot1, from the LOV2 domain to the NTP binding site (Fig. 6). A possible way of light-induced activation in YtvA may involve conformationally driven changes in the NTP-binding affinity or hydrolysis, and, accompanied with the interaction with a kinase, this may represent the signaling switch. In this respect, YtvA, being highly soluble (contrary to phototropins (Christie et al., 1998)) and stable as a full protein, could become a model system for the study of light-induced conformational changes and intradomain communication in phototropins.

The physiological role of the blue-light-induced reaction in *B. subtilis* YtvA is presently unknown. It was recently reported that YtvA is a positive regulator in the activation of the general stress transcription factor σ^B , but the environmental input sensed by its LOV domain has remained undetermined and its precise function unclarified (Akbar et al., 2001). We propose here that the environmental input can be blue light. Although photosensory responses have not been described for *B. subtilis*, two growth patterns induced by long-wavelength UV (310–400 nm) irradiation have been observed (Neicu et al., 2000; Delprato et al., 2001). YtvA would fulfill the spectral characteristics for being involved in this photobehavior, although this requires experimental assessment.

Bacillus subtilis is a common, nonphotosynthetic soil organism, that experiences during its life-cycle a variety of growth-limiting stresses and environmental signals. The presence of a protein having the photochemical characteristics of higher plants phototropins, is certainly surprising and intriguing. The large sequence homology and the fact that YtvA resembles a fragment of phot1, suggest that vertical gene transfer may have occurred between *B. subtilis* and plants, obviously facilitated by living in the same (or

closely related) environment. The way phototropins sense, by means of an oxydized flavin, and respond to blue-light, by undergoing an apparently extremely simple photocycle (Swartz et al., 2001), has certainly established a new paradigm among photosensors. The fact that the paradigm has been preserved between plants and bacteria supports the idea that the ways living organisms sense and respond to light, a basic source of energy and information, have been optimized by evolution and conserved basically unchanged among different taxa. In line with this concept, it has been recently showed that photoreceptors similar to archaeal rhodopsins, also exist in fungi (Bieszke et al., 1999) and in microscopic plankton organisms (Béjà et al., 2000). To our knowledge, however, ours are the first studies indicating that phototropin-related blue-light receptors may exist also in prokaryotes, besides constituting a steadily growing family in plants.

A.L. acknowledges a post-doctoral fellowship at the University of Parma, Italy. E.P. is a post-doctoral INFM fellow.

We thank Prof. Jäger (University of Bochum) for kindly providing *B. subtilis* DNA. The technical help of Gudrun Klihm and Helene Steffen is greatly appreciated. We thank Ingo Lindner for help with the TLC analysis. We are particularly grateful to Prof. S.E. Braslavsky for the use of the time-resolved spectroscopic facilities, for many hours of helpful discussion, and for her support.

REFERENCES

- Abbruzzetti, S., C. Viappiani, D. H. Murgida, R. Erra-Balsells, and G. M. Bilmes. 1999. Non-toxic, water-soluble photocalorimetric reference compounds for UV and visible excitation. *Chem. Phys. Lett.* 304: 167–172.
- Akbar, S., T. A. Gaidenko, C. M. Kang, C. M. M. O'Reilly, K. M. Devine, and C. W. Price. 2001. New family of regulators in the environmental signaling pathway which activates the general stress transcription factor of *Bacillus subtilis*. *J. Bacteriol.* 183:1329–1338.
- Altschul, S. F., T. L. Madden, A. A. Schaffer, J. Zhang, Z. Zhang, and D. J. Lipman. 1997. Gapped BLAST and PSI-BLAST: a new generation of protein database search programs. *Nucleic Acids Res.* 25:3389–3402.
- Aravind, L., and E. V. Koonin. 2000. The STAS domain: a link between anion transporters and antisigma-factor antagonists. *Curr. Biol.* 10: R53–R55.
- Béjà, O., L. Aravind, E. V. Koonin, M. T. Suzuki, A. Hadd, L. P. Nguyen, S. B. Jovanovich, C. M. Gates, R. A. Feldman, J. L. Spudich, E. N. Spudich, and E. F. DeLong. 2000. Bacterial rhodopsin: evidence for a new type of phototrophy in the sea. *Science*. 289:1902–1906.
- Bieszke, J. A., E. N. Spudich, K. L. Scott, K. A. Borkovich, and J. L. Spudich. 1999. A eukaryotic protein, NOP-1, binds retinal to form an archaeal rhodopsin-like photochemically reactive pigment. *Biochemistry*. 38:14138–14145.
- Borgstahl, G. E., D. R. Williams, and E. D. Getzoff. 1995. 1.4 Å structure of photoactive yellow protein, a cytosolic photoreceptor: unusual fold, active site, and chromophore. *Biochemistry*. 34:6278–6287.
- Braslavsky, S. E., and G. E. Heibel. 1992. Time-resolved photothermal and photoacoustic methods applied to photoinduced processes in solution. *Chem. Rev.* 92:1381–1410.
- Briggs, W. R., C. F. Beck, A. R. Cashmore, J. M. Christie, J. Hughes, J. A. Jarillo, T. Kagawa, H. Kanegae, E. Liscum, A. Nagatani, K. Okada, M. Salomon, W. Rüdiger, T. Sakai, M. Takano, M. Wada, and J. C. Watson. 2001. The phototropin family of photoreceptors. *Plant Cell*. 13:993–997.

- Christie, J. M., P. Reymond, G. K. Powell, P. Bernasconi, A. A. Raibekas, E. Liscum, and W. R. Briggs. 1998. Arabidopsis NPH1: a flavoprotein with the properties of a photoreceptor for phototropism. *Science*. 282: 1698–1701.
- Christie, J. M., M. Salomon, K. Nozue, M. Wada, and W. R. Briggs. 1999. LOV (light, oxygen, or voltage) domains of the blue-light photoreceptor phototropin (nph1): binding sites for the chromophore flavin mononucleotide. *Proc. Natl. Acad. Sci. U.S.A.* 96:8779–8783.
- Crosson, S., and K. Moffat. 2001. Structure of a flavin-binding plant photoreceptor domain: insights into light-mediated signal transduction. *Proc. Natl. Acad. Sci. U.S.A.* 98:2995–3000.
- Delprato, A., A. Samadani, and A. Kudrolli. 2001. Swarming ring patterns in bacterial colonies exposed to ultraviolet radiation. *Phys. Rev. Lett.* 87:158102.
- Hoff, W. D., P. Dux, K. Hard, B. Devreese, I. M. Nugteren-Roodzant, W. Crielaard, R. Boelens, R. Kaptein, and J. V. Beeumen. 1994. Thiol ester-linked *p*-coumaric acid as a new photoactive prosthetic group in a protein with rhodopsin-like photochemistry. *Biochemistry*. 33: 13959–13962.
- Losi, A., A. A. Wegener, M. Engelhard, W. Gärtner, and S. E. Braslavsky. 2000. Aspartate 75 mutation in sensory rhodopsin II from *Natronobacterium pharaonis* does not influence the production of the K-like intermediate, but strongly affects its relaxation pathway. *Biophys. J.* 78: 2581–2589.
- Malkin, S., M. S. Churio, S. Shochat, and S. E. Braslavsky. 1994. Photochemical energy storage and volume changes in the microsecond time range in bacterial photosynthesis: a laser-induced optoacoustic study. *J. Photochem. Photobiol. B. Biol.* 23:79–85.
- Neicu, T., A. Pradhan, D. A. Larochelle, and A. Kudrolli. 2000. Extinction transition in bacterial colonies under forced convection. *Phys. Rev.* 62:1059–1062.
- Ruddat, A., P. Schmidt, C. Gatz, S. E. Braslavsky, W. Gärtner, and K. Schaffner. 1997. Recombinant type A and B phytochromes from potato: transient absorption spectroscopy. *Biochemistry*. 36:103–111.
- Rudzki, J. E., J. L. Goodman, and K. S. Peters. 1985. Simultaneous determination of photoreaction dynamics and energetics using pulsed, time-resolved photoacoustic calorimetry. *J. Am. Chem. Soc.* 107: 7849–7854.
- Rudzki-Small, J., L. J. Libertini, and E. W. Small. 1992. Analysis of photoacoustic waveforms using the nonlinear least square method. *Biophys. Chem.* 41:29–48.
- Sakai, M., and H. Takahashi. 1996. One-electron photoreduction of flavin mononucleotide: time-resolved resonance Raman and absorption study. *J. Mol. Struct.* 379:9–18.
- Salomon, M., J. M. Christie, E. Knieb, U. Lempert, and W. R. Briggs. 2000. Photochemical and mutational analysis of the FMN-binding domains of the plant blue light receptor, phototropin. *Biochemistry*. 39: 9401–9410.
- Salomon, M., W. Eisenreich, H. Dürr, E. Schleicher, E. Knieb, and V. Massey. 2001. An optomechanical transducer in the blue light receptor phototropin from *Avena sativa*. *Proc. Natl. Acad. Sci. U.S.A.* 98: 12357–12361.
- Swartz, T. E., S. B. Corchnoy, J. M. Christie, J. W. Lewis, W. R. Szundi, W. R. Briggs, and R. A. Bogomolni. 2001. The photocycle of a flavin-binding domain of the blue light photoreceptor phototropin. *J. Biol. Chem.* 276:36493–36500.
- van den Berg, P. W., J. Widengren, M. A. Hink, R. Rigler, and A. G. Visser. 2001. Fluorescence correlation spectroscopy of flavins and flavoenzymes: photochemical and photophysical aspects. *Spectrochim. Acta A: Mol. Biomol. Spectrosc.* 57:2135–2144.
- van Gunsteren, W. F., S. R. Billeter, A. A. Eising, P. H. Hünenberger, P. Krüger, A. E. Mark, W. R. P. Scott, and I. G. Tironi. 1996. Biomolecular Simulation: The GROMOS96 Manual and User Guide. Vdf Hochschulverlag AG an der ETH Zürich, Zürich, Switzerland.
- van Brederode, M. E., T. Gensch, W. D. Hoff, K. J. Hellingwerf, and S. E. Braslavsky. 1995. Photoinduced volume change and energy storage associated with the early transformations of the photoactive yellow protein from *Ectothiorhodospira halophila*. *Biophys. J.* 68:1101–1109.
- Vriend, G. 1990. WHAT IF: a molecular modeling and drug design program. *J. Mol. Graph.* 8:52–56.
- Zhulin, I. B., B. L. Taylor, and R. Dixon. 1997. PAS domain S-boxes in archaea, bacteria and sensors for oxygen and redox. *Trends Biochem. Sci.* 22:331–333.